EVALUATION OF THE INFLUENCE OF LEAFLET STIFFENING ON LEAFLET STRESSES OF PORCINE BIOPROSTHETIC VALVES USING A FINITE ELEMENT MODEL

Hani N. Sabbah, Mohamed S. Hamid, Paul D. Stein

Henry Ford Heart and Vascular Institute, 2799 West Grand Boulevard, Detroit, Michigan 48202 USA

Abstract. The magnitude and distribution of mechanical stresses acting on the closed cusps of porcine bioprosthetic valves were estimated using a finite element model. Leaflet stresses were calculated using reported stress-strain properties of glutaraldehyde processed normal porcine valves and stress-strain properties of porcine valve leaflets stiffened by fatigue cycling (658 x 10 cycles). In the normal leaflet, at a pressure of 80 mm Hg, stresses were highest near the commissures (140 kPa), decreased near the center of the leaflet (110 kPa) and were lowest near the base of the leaflet (30 kPa). With increased leaflet stiffening, stresses near the commissures remained relatively unchanged (140 kPa). Stresses near the center of the leaflet, however, increased markedly (170 kPa). With increased leaflet stiffening, stresses near the base of the leaflet remained the lowest (60 kPa). The development of a site of stress concentration near the center of the leaflet following leaflet stiffening, may offer a clue to the etiology of leaflet perforations reported to occur in the central region of leaflets of degenerated porcine bioprosthetic valves.

Keywords. Porcine bioprosthetic heart valves; finite element method; modelling of cardiac valves.

INTRODUCTION

The spontaneous degeneration of porcine bioprosthetic valves (PBV) is accompanied by calcification, cuspal disruption and often, increased stiffening of the valvular leaflets. Both calcification and cuspal disruption have been attributed, in part, to mechanical stresses (Ishihara et al, 1981; Thubrikar et al, 1983). Cuspal disruption, characterized by tears and perforations, has been suggested to develop in PBVs as the final consequence of tissue failure. Connective tissue failure is thought to develop in areas in which mechanical forces are exerted in a highly localized manner (Ishihara et al, 1981). Mechanical stresses are also believed by some to be an initiating factor of calcification of PBVs (Thubrikar et al, 1983).

Direct measurement of mechanical stresses on valvular leaflets, whether bioprosthetic or natural, is extremely difficult or impossible. Experimental studies using radiopaque markers sewn to the leaflet surface have been used to estimate leaflet stresses during systole and diastole for both natural aortic valves and PBVs in the aortic position (Thubrikar et al, 1980). An alternative approach to the direct measurement of leaflet stresses is the use of numerical models that can account for changes of leaflet geometry and material properties (Christie and Medland, 1982). The purpose of this study was to determine if the increased stiffness of degenerated PBVs is one modality that leads to increased mechanical stresses. Leaflet stresses were determined using the finite element method.

METHODS

Assumptions

In developing the model, several assumptions were made to simplify the numerical solution. The 3 PBV leaflets were assumed to be equal in size, symmetrical and uniformly thick (0.6 mm). The deformation of the valve anulus under load (pressure) was neglected. The valve tissue was considered isotropic, with a Poisson's ratio of 0.45. Bending effects were neglected in comparison to in-plane membrane forces and the stent was assumed to be rigid.

The Model

The geometry of the stent-mounted porcine aortic valve leaflets is complex even in the relaxed state (no pressure difference across the closed cusps). Based on our examination of various types of PBVs, the relaxed leaflet shape was modelled as one-half of an elliptic-paraboloid. The anular diameter of the valve used in the model was 27 mm. The height of the stent posts was 19.0 mm and the surface area of a single leaflet was 5.77 cm^2.

The geometry of the PBV, as viewed from directly above the outflow side of the valve, is shown in Figure 1. The leaflet is firmly attached to the support structure along the line ABC. The assumption was made that the cloth and sutures, in addition to the stent itself, are rigid. Although this is not exactly the case, the deformation of these components under pressure can reasonably be expected to be negligible compared with that of the leaflets themselves (Christie and Medland, 1982).

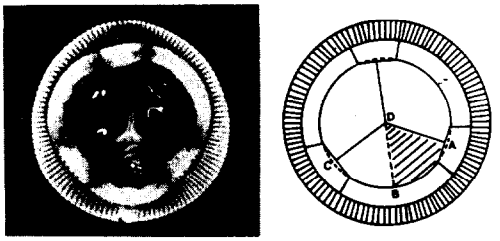

Fig. 1

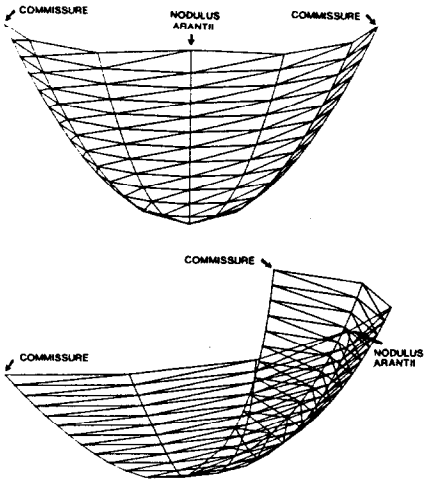

Fig. 2

Finite Element Discretization

Because of assumptions of symmetry, only one-half of 1 leaflet was considered for analysis. The finite element discretization for the entire leaflet is shown in Figure 2. Triangular membrane shell elements were used in the analysis. The discretization resulted in 138 elements and 78 nodes.

Element Formulation

In large deformation nonlinear analysis, the element equilibrium should be established in its current configuration during deformation. An updated Lagrangian approach was adopted in the formulation (Bathe, 1982). In the incremental procedure, the solution at time t must be known, and the solution at a discrete time t + Δt satisfies the equilibrium equation

$$ {}^{t+\Delta t}R - {}^{t+\Delta t}F = 0 \qquad (1) $$

where the vector R represents the externally applied load at time t + Δt and the vector ${}^{t+\Delta t}F$ lists the nodal forces that correspond to the element stresses in this configuration.

Since the solution is known at time t, the element equilibrium equations in incremental form can be written as follows (Zienkiewicz, 1977)

$$ [K]_T^e \{u\}^e = \{\Delta P\}^e \qquad (2) $$

where $[K]_T^e$ represents the tangent stiffness matrix, $\{u\}^e$ represents the vector of incremental nodal displacements, and $\{\Delta P\}^e$ is the increment in nodal point forces corresponding to the increment in element stresses and displacements from time t to t + Δt.

The tangent element stiffness matrix $[K]_T^e$ was obtained by using the principle of virtual displacements. Definition of the second Piola-Kirchhoff stress and the Lagrangian strain was used in the derivation of element matrices.

For a flat triangular membrane element which undergoes large deformation, large rotation, but small strain, the incremental strains are given as follows:

$$ \{\epsilon\} = [B]_l \{u\}^e + [B]_n \{u\}^e \qquad (3) $$

where $[B]_l$ and $[B]_n$ are the linear and nonlinear part of the strain displacement matrix and $\{u\}^e$ are the incremental nodal in plane and normal displacements.

Using the variational principle, the element tangent stiffness matrix is obtained as follows:

$$ [K]_T^e = \int \Big([B]_w^T [\sigma] [B]_w + [B]_l^T [D] [B]_l + [B]^{*T}_n [D] [B]_l + [B]_l^T [D] [B]^*_n + [B]^{*T}_n [D] [B]^*_n \Big) dv \qquad (4) $$

The matrices $[B]_w$, $[B]_l$, and $[B]_n^{*T}$ are obtained from the variations of strains $\delta(\epsilon)_l$, and $\delta(\epsilon)_n$ as follows:

$$ \delta(\epsilon)_l = [B]_l \, \delta\{u\}^e \qquad (5) $$

$$ \delta(\epsilon)_n = [B]^*_n \, \delta\{u\}^e \qquad (6) $$

$$ \delta^2 \{\epsilon\}_n^T \{\sigma\} = \delta\{u\}^{eT} [B]_w^T [\sigma] [B]_w \delta\{u\}^e \qquad (7) $$

where $\{\sigma\}$ is the element stress vector, $[\sigma]$ is the element stress tensor and [D] is the material property matrix.

The deformation dependent loading condition also contributes to the tangent stiffness coefficients. This component is nonsymmetric, and was, therefore, computationally inefficient to handle. However, for small incremental pressure, this nonsymmetric contribution can be neglected. In general, evaluation of the constitutive matrix [D] involves transformations [9]. Because the formulation was based upon the hypothesis of large deformation, large rotation, and small strain, and the material was assumed to be isotropic, the transformations would not change the components of the constitutive matrix. Therefore, the generalized Hooke's law was employed in the computation of the material property matrix.

Boundary Conditions

As the leaflet deforms under pressure, the free margin (AC in Fig. 3) comes in contact with the neighboring leaflet. Once contact is made, pressure forces oppose each other at contact points. The deformed geometry was obtained after computation of the displacements at any load level. The nodal coordinates of the deformed geometry were checked for any point that contacted the plane AC at $\theta = 60^0$. The nodal points which were in contact with the plane AC or cross the plane AC were assigned as boundary points in the next load step. It was also assumed that

any point which came in contact with the neighboring leaflet was always in contact during subsequent deformations.

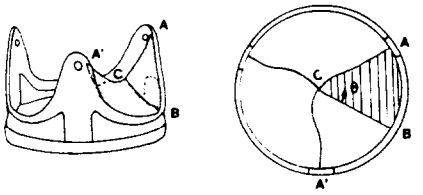

Fig. 3

Analysis

The analysis was carried out using, in part, a minicomputer (Hewlett-Packard 21MX System). The system had an RTE IV B operating system with 160 K word of total memory of which 20 K memory partition was available to the user at any time. The minicomputer was used for (i) finite element mesh generation, (ii) plotting of the deformed leaflet shapes, and (iii) plotting of stress distribution. The finite element equations were solved using an Amdahl 470/V8 mainframe computer.

The solution of the finite element equations was obtained by increasing the pressure at discrete increments from 0 mm Hg to 160 mm Hg. The pressure load increments were applied to the outflow surface of the leaflet while the inflow surface was assumed to be free from any applied pressure. The stress-strain curve for the porcine bioprosthetic leaflets was based upon experiments by others [Broom, 1978]. The Young's modulus was calculated based upon the stress level of the element in the previous load increment. The stress-strain curve was linearized into five segments (Fig. 4). The computer code picked up the Young's modulus E ($E_1, E_2, \ldots, E_5$) corresponding to the total stress level of the element in the local element coordinate system. These values were used to compute the constitutive matrix (D). After each incremental solution, the equilibrium of forces was checked. If the equilibrium condition was not satisfied, additional iterations were performed before the next incremental load was applied. An initial equibiaxial stress of 0.002 kPa was assumed in all the elements in order to smooth out the surface [Christie and Medland, 1982]. The first load increment was 0.013 kPa (0.1 mm Hg) and the subsequent increments were 0.025 kPa, 0.039 kPa, 0.052 kPa, and 0.13 kPa. Then the load was incremented by 0.26 kPa up to 1.3 kPa pressure and after that it was increased by 1.3 kPa.

The magnitude and distribution of the maximal principal normal stresses and maximal shear stresses were obtained for the following conditions: simulated normal porcine leaflet; and simulated stiffened leaflet.

To determine the effects of leaflet stiffening on the magnitude and distribution of stresses, the stress-strain properties of glutaraldehyde-treated porcine leaflets subjected to 648 X 10^6 in vitro fatigue cycles were used (Broom, 1978). The stress-strain curve for the normal PBV leaflets used in the study was also based upon experiments by Broom (1978).

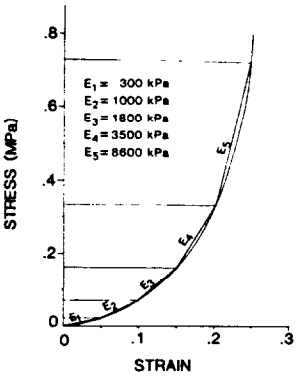

Fig. 4

RESULTS

The Normal PBV Leaflet

In the normal gluteraldehyde-treated porcine aortic valve leaflet, both the maximal principal normal stresses and maximal shear stresses were higher near the leaflet commissures in comparison to the main body of the leaflet (Table I).

Table I

Maximal Principal Normal Stress (kPa)

Pressure (mm Hg)	Commissure	Center	Base
80	140	110	40
100	160	130	60
120	200	140	40
140	240	170	60
160	260	190	70

Maximal Shear Stress (kPa)

Pressure (mm Hg)	Commissure	Center	Base
80	70	50	30
100	80	60	40
120	100	70	30
140	120	80	40
160	130	90	50

The stresses on the leaflet increased when overall leaflet tissue stiffening was simulated (Table II). Stiffening resulted in a site of maximal principal normal stress concentration near the center of the leaflet. At 80 mm Hg, the maximal principal normal stress near the center of the leaflet increased 55% when the leaflet was stiff in comparison to the normal leaflet. Shear stresses were also higher at the center of the leaflet when stiffening was introduced (Table II).

Table II

Maximal Principal Normal Stress (kPa)

Pressure (mm Hg)	Commissure	Center	Base
80	140	170	60
100	180	220	70
120	220	260	80
140	280	280	90
160	310	320	100

Maximal Shear Stress (kPa)

Pressure (mm Hg)	Commissure	Center	Base
80	90	70	30
100	100	80	40
120	120	100	40
140	130	110	50
160	150	130	60

In both the normal PBV leaflet and the stiffened leaflet the maximal principal normal stress and shear stress increased with increasing load on the closed valve (increasing pressure) (Table I and II).

DISCUSSION

Numerical models designed to simulate certain anatomic systems suffer in accuracy as a result of inherent assumptions necessary to obtain a solution. As with any model, some of the assumptions made in this study are justifiable, while others are tenuous. The leaflets of a PBV are usually of different size and seldom symmetrical. Lack of symmetry, however, does not significantly affect the mechanics of statically loaded valves (Christie and Medland, 1982). The leaflet thickness of a PBV is not uniform, and variability among different specimens is likely. Using human aortic valves, Clark and Finke (1974) showed that the leaflet thickness was not uniform and varied markedly between the relaxed state and the pressure stressed state. A topographic determination of PBV leaflet thickness in the relaxed or stressed state is yet to be made.

A Poisson's ratio of 0.45 was used in our model to approach conditions of incompressibility typical of biologic material. Such material is also invariably anisotropic. Stress-strain properties of leaflets of PBVs differ between the circumferential and radial directions. Nevertheless, the assumption of isotropy was made for simplicity. Christie and Medland (1982) simulated anisotropy in cusps of PBVs by reinforcing the leaflets with circumferentially aligned fibers. This method of simulating anisotropy gives the leaflet more compliance radially than circumferentially and is qualitatively in agreement with natural untreated tissue (Swanson and Clark, 1974). The extent to which such an approach may be applicable, however, to the glutaraldehyde-fixed tissue remains uncertain. Glutaraldehyde tissue fixation causes a marked reduction in radial compliance of the tissue (Broom and Christie, 1982). The pressure at which the tissue is fixed also can influence the radial and circumferential compliance of the porcine leaflet (Broom and Christie, 1982).

Generally, the support stent of a PBV is made from thin polypropylene, which is somewhat flexible. In our model the stent was assumed rigid to minimize complexity. Studies by Thubrikar et al, (1982), using radiopaque markers placed at the tip of stent posts of PBVs implanted in the aortic position of calves, showed that the stent posts did not flex during any part of the cardiac cycle. However, their technique cannot detect movement of the stent posts of less than 0.5 mm.

In this study, leaflet stresses on the closed valves increased in direct response to an increase in the applied pressure. This would suggest that a PBV in the mitral position would experience higher mechanical stresses because of higher pressure during systole acting on the closed mitral valve than pressure during diastole acting on the closed aortic valve. On this basis, valves in the tricuspid position may experience the least level of stress. Several studies have shown a greater frequency of degeneration among PBVs in the mitral position in comparison to PBVs in the aortic or tricuspid positions (Schoen, et al, 1983; Warnes et al, 1983; Cohen et al, 1984).

The model predicted higher leaflet stresses near the commissures which increased slightly after stiffening of the leaflet. Morphologic examination of degenerated PBVs showed a high incidence of tears and calcification of this region (Stein et al, 1985; Milano et al, 1984).

When the overall stiffness of the porcine leaflet was increased in our model to stimulate the stiffening observed in PBVs after long periods of implantation, a site of stress concentration developed near the center of the leaflet. The development of this new site of stress concentration after leaflet stiffening may offer a clue to the mechanisms of large oval perforations, which have been reported to occur in the central regions of leaflets of degenerated PBVs (Ishihara et al, 1981).

The magnitude and distribution of stresses on PBV leaflets reported in this study were limited to those that may occur at a time when the valve is closed and are by no means representative of stresses throughout the cardiac cycle. Mechanical stresses that arise from the opening and closing action of the leaflets were not considered in this model. Thubrikar et al (1982) reported high compressive stresses that result from flexion along the leaflet attachment. Ishihara et al (1981) suggested that the pattern of opening and closure of the cusps of PBVs, together with the straightening of the waviness of the collagen fibrils, tend to result in bending stresses, which become localized to certain points along the free edges. Such bending stresses were thought to result in tears along the free edge of the cusp. The stresses estimated in this study may be considered additive to stresses that result from the opening and closing action of bioprosthetic leaflets.

CONCLUDING REMARKS

In conclusion, an estimation of stresses on the closed cusps of a PBV leaflet using a numerical model indicate that the magnitude of

stresses is dependent upon the level of pressure applied to the closed valve. Increased overall stiffening of PBV leaflets secondary to prolonged implantation is predicted by the model to increase the magnitude of stresses and create new sites of stress concentration.

REFERENCES

Bathe, K.J. (1982). Finite Element Procedures in Engineering Analysis. Prentice-Hall, Englewood Cliffs, N.J.

Broom, N.D. (1978). Fatigue-induced damage in glutaraldehyde-preserved heart valve tissue. J. Thorac. Cardiovasc. Surg., 76, 202-211.

Broom, N., G.W. Christie (1982). The structure/function relationship of fresh and glutaraldehyde-fixed aortic valve leaflets. In: L.H. Cohen, V. Gallucci, eds. Cardiac Bioprosthesis. New York: Yorke Medical Books. pp. 476-491.

Christie, G.W., I.C. Medland (1982). A non-linear finite element stress analysis of bioprosthetic heart valves. In: R.H. Gallagher, ed. Finite Elements in Biomechanics. New York: Wiley & Sons, pp. 153-179.

Clark, R.E., E.H. Finke (1974). Scanning and light microscopy of human aortic leaflets in stressed and relaxed states. J. Thorac. Cardiovasc. Surg., 67, 792-804.

Cohen, S.R., M.A. Silver, C.L. McIntosh, and W.C. Roberts (1984). Comparison of late (62 to 140 months) degenerative changes in simultaneously implanted and explanted porcine (Hancock) bioprotheses in the tricuspid and mitral valve positions in six patients. Am. J. Cardiol., 53, 1599-1602.

Ishihara, T., V.J. Ferrans, S.W. Boyce, M. Jones, and W.C. Roberts (1981). Structure and classification of cuspal tears and perforations in porcine bioprosthetic cardiac valves implanted in patients. Am. J. Cardiol., 48, 665-678.

Milano, A., U. Bortolotti, E. Talenti, C. Valfre, E. Arbustini, M. Valente, A. Muzzucco, V. Gallucci, and G. Thiene (1984). Calcific degeneration as the main cause of porcine bioprosthetic valve failure. Am. J. Cardiol., 53, 1066-1070.

Schoen, F.J., J.J. Collins, Jr., and L.H. Cohn (1983). Long-term failure rate and morphologic correlation in porcine bioprosthetic heart valves. Am. J. Cardiol., 51, 957-964.

Stein, P.D., S.R. Kemp, J.M. Riddle, M.W. Lee, J.W. Lewis, Jr., and D.J. Magilligan, Jr. (1985). Relation of calcification to torn leaflets of spontaneously degenerated porcine bioprosthetic valves. Ann. Thorac. Surg., 40, 175.

Swanson, M., R.E. Clark (1974). Dimensions and geometric relationships of the human aortic valve as a function of pressure. Circ. Res., 35, 871-882.

Thubrikar, M., W.C. Piepgrass, J.D. Deck, and S.P. Nolan (1980). Stresses of natural versus prosthetic aortic valve leaflets in vivo. Ann. Thorac. Surg., 30, 230-239.

Thubrikar, M.J., J.R. Skinner, R.T. Eppink, and S.P. Nolan (1982). Stress analysis of porcine bioprosthetic heart valves in vivo. J. Biomed. Mat. Res., 16, 811-826.

Thubrikar, M.J., J.D. Deck, J. Aouad, and S.P. Nolan (1983). Role of mechnical stress in calcification of aortic bioprosthetic valves. J. Thorac. Cardiovasc. Surg., 86, 115-125.

Warnes, C.A., M.L. Scott, G.M. Silver, C.W. Smith, V.J. Ferrans, and W.C. Roberts (1983). Comparison of late degenerative changes in porcine bioprostheses in the mitral and aortic valve position in the same patient. Am. J. Cardiol., 51, 965-968.

Zienkiewicz, O.C. (1977). The Finite Element Methods, 3rd ed., McGraw-Hill, London.